Title

A synapse-specific refractory period for plasticity at individual dendritic spines

Journal

Proceedings of the National Academy of Sciences of the United States of America, 122(2)

ISSN

0027-8424

Authors

Flores, Juan C

Sarkar, Dipannita

Zito, Karen

Publication Date

2025-01-14

DOI

10.1073/pnas.2410433122

Peer reviewed

PNAS RESEARCH ARTICLE | NEUROSCIENCE OPEN ACCESS

A synapse-specific refractory period for plasticity at individual dendritic spines

Juan C. Flores[a], Dipannita Sarkar[a], and Karen Zito[a,1]

Edited by Yi Zuo, University of California Santa Cruz, Santa Cruz, CA; received May 24, 2024; accepted December 4, 2024 by Editorial Board Member Yishi Jin

How newly formed memories are preserved while brain plasticity is ongoing has been a source of debate. One idea is that synapses which experienced recent plasticity become resistant to further plasticity, a type of metaplasticity often referred to as saturation. Here, we probe the local dendritic mechanisms that limit plasticity at recently potentiated synapses. We show that recently potentiated individual synapses exhibit a synapse-specific refractory period for further potentiation. We further found that the refractory period is associated with reduced postsynaptic CaMKII signaling; however, stronger synaptic activation fully restored CaMKII signaling but only partially restored the ability for further plasticity. Importantly, the refractory period is released after one hour, a timing that coincides with the enrichment of several postsynaptic proteins to preplasticity levels. Notably, increasing the level of the postsynaptic scaffolding protein, PSD95, but not of PSD93, overcomes the refractory period. Our results support a model in which potentiation at a single synapse is sufficient to initiate a synapse-specific refractory period that persists until key postsynaptic proteins regain their steady-state synaptic levels.

dendritic spine | synaptic plasticity | metaplasticity | PSD-95 | two-photon imaging

Significance

A refractory period in which newly modified synaptic connections are unable to undergo further plasticity is a proposed mechanism through which newly formed memories can be preserved at the synaptic level while brain plasticity is ongoing. Here, we provide insights into the spatiotemporal signaling mechanisms that regulate the establishment and maintenance of a refractory period for plasticity at individual excitatory synapses in the hippocampus, a region of the brain vital for learning and memory. Our results have implications in the identification of molecular targets that could serve to improve learning outcomes associated with disease.

Learning and memory are thought to rely upon long-term changes in neural circuit connections, both via alterations in the strength of existing synapses and through formation of new synapses (1–3). One challenge for synaptic models of learning and memory has been how synapses can be both plastic, in order to encode new memories, and stable, in order to retain old memories (4–11). A prominent hypothesis posits that synaptic connections that have recently been strengthened during learning are protected from further modification (12–14). Indeed, there is evidence that when animals learn two distinct tasks over a close period of time, nonoverlapping populations of synapses encode the two distinct tasks (2, 15).

An important component of synaptic learning models therefore would be mechanisms that support selection of nonoverlapping sets of labile synapses to encode distinct tasks learned close in time. One such mechanism could be through the existence of a period of time in which recently potentiated synapses are unable to undergo further potentiation; this type of metaplasticity has often been referred to as saturation of plasticity (12, 16, 17). Indeed, in vitro studies at the circuit level have shown that recently potentiated hippocampal circuits are unable to undergo further potentiation within the first few hours after potentiation (18–21). Furthermore, in vivo studies have shown that after inducing saturation of potentiation in the hippocampus of live rats, learning is impaired compared to control animals (16). However, the cellular and molecular mechanisms that inhibit further plasticity at recently potentiated individual synapses, and the spatial and temporal scales over which they act, are not well understood.

Here, we show that prior potentiation at individual dendritic spines on dendrites of hippocampal CA1 neurons is sufficient to initiate a refractory period that prevents additional structural and functional plasticity. We further show that the refractory period is limited to synapses receiving prior potentiation, and that it is postsynaptically initiated and accompanied by reduced postsynaptic activation of CaMKII. Increasing the strength of the potentiating stimulus at 30 min is not sufficient to fully overcome the refractory period at individual synapses; however, it is fully released within 60 min. Finally, we show that increasing levels of the postsynaptic scaffolding protein PSD95, but not of PSD93, is sufficient to release the refractory period, such that previously potentiated synapses are again able to exhibit robust plasticity at a time when they would typically be refractory.

Results

Individual Potentiated Spine Synapses are Refractory to Further Plasticity. To test whether recently potentiated individual synapses on hippocampal CA1 neurons are restricted from further plasticity, our strategy was to induce long-term potentiation

Author affiliations: [a]Center for Neuroscience, University of California, Davis, CA 95618

Author contributions: J.C.F. and K.Z. designed research; J.C.F. and D.S. performed research; J.C.F. and D.S. analyzed data; and J.C.F. and K.Z. wrote the paper.

The authors declare no competing interest.

This article is a PNAS Direct Submission. Y.Z. is a guest editor invited by the Editorial Board.

[1]To whom correspondence may be addressed. Email: kzito@ucdavis.edu.

This article contains supporting information online at https://www.pnas.org/lookup/suppl/doi:10.1073/pnas.2410433122/-/DCSupplemental.

Published January 7, 2025.

(LTP) at a single target spine and then test whether further potentiation could be induced at the same target spine 30 min later (Fig. 1*A*). After two baseline images, individual spines on EGFP-expressing CA1 neurons in slice cultures were stimulated with high-frequency uncaging of MNI-glutamate (HFU), which has been shown to induce concurrent long-term increases in

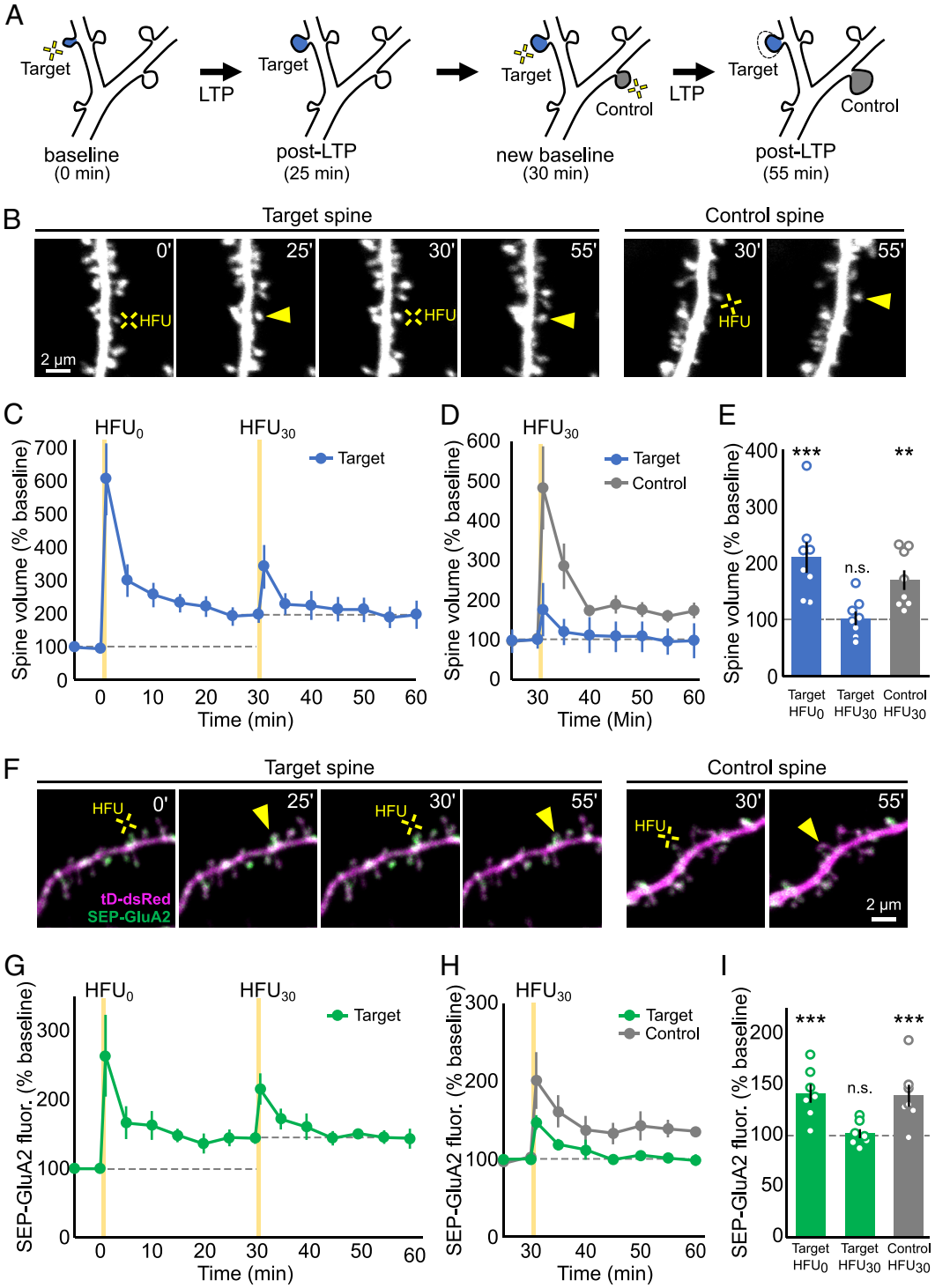

Fig. 1. A single LTP-inducing stimulus initiates a refractory period for long-term growth and synaptic strengthening at individual dendritic spines (*A*) Schematic of the experimental approach. An individual dendritic spine (target) was stimulated (yellow crosses) to induce LTP and then imaged every 5 min. At 30 min, the target spine was stimulated again along with a previously unstimulated, size-matched control spine (control) on a different dendrite of the same cell. (*B*) Images of dendrites from an EGFP-transfected hippocampal CA1 pyramidal neuron directly prior to and 25 min after HFU_0 and HFU_{30} at target (*Left* images) and control (*Right* images) spines. (*C–E*) The initial HFU stimulus (HFU_0) resulted in long-term growth of target spines (filled blue circles/bars; n = 8 spines/cells), but an identical HFU at 30 min (HFU_{30}) did not drive additional growth. A size-matched control spine on the same cell grew in response to HFU_{30} (gray circles/bar; n = 8 spines/cells). Target spine data in D are from C renormalized to the new baseline. (*F*) Images of dendrites from a CA1 pyramidal neuron transfected with SEP-GluA2 (green) and tDimer-dsRed (magenta) directly prior to and 25 min after HFU_0 and HFU_{30} at target (*Left* images) and control (*Right* images) spines. (*G–I*) An initial HFU stimulus (HFU_0) resulted in a long-term increase in surface expression of SEP-GluA2 in target spines (filled green circles/bars; n = 7 spines/cells), but an identical HFU at 30 min (HFU_{30}) did not drive an additional increase. In contrast, HFU_{30} drove a long-term increase in surface SEP-GluA2 on a size-matched control spine on the same cell (gray circles/bar; n = 7 spines/cells). Target spine data in *H* are from *G* renormalized to the new baseline. Data are represented as mean ± SEM. Statistics: two-way ANOVA with the Bonferroni test. $^{**}P < 0.01$, $^{***}P < 0.001$. See also *SI Appendix*, Fig. S1.

synaptic strength and spine size (22, 23). As expected, following an initial HFU at time 0 (HFU_0), we observed that stimulated target spines exhibited a long-term increase in size (Fig. 1 *B*, *C*, and *E*; 210% ± 20%; $P < 0.001$). Notably, an identical HFU stimulus at the same target spine 30 min later (HFU_{30}) induced no further long-term growth (Fig. 1 *B–E* and *SI Appendix*, Fig. S1 *A–C* and Table S1; 102% ± 12%; $P > 0.99$). Importantly, previously unstimulated, size-matched (*SI Appendix*, Fig. S1*D*) control spines on different dendrites of the same cells exhibited a robust long-term increase in size in response to HFU_{30} (Fig. 1 *B*, *D*, and *E*; 170% ± 18%; $P < 0.01$), supporting that the lack of plasticity observed in the restimulated target spine was not due to either i) a decay in ability to undergo plasticity after 30 min in the bath chamber and/or ii) the increased spine size following the first round of plasticity. Our results demonstrate that prior potentiation initiates a refractory period for further plasticity at individual dendritic spines.

In addition to a long-term increase in spine size, potentiation at single spines also drives a long-term increase in surface AMPARs (22–24). To examine whether insertion of surface AMPARs also exhibits a refractory period following potentiation at single dendritic spines, we transfected CA1 neurons with super ecliptic pHluorin (SEP)-tagged GluA2 to monitor surface expression of AMPARs (24–26) along with tDimer-dsRed as a red cell fill (Fig. 1*F*). Importantly, by monitoring the red cell fill, we observed that the presence of SEP-GluA2 did not alter establishment of the refractory period for plasticity (*SI Appendix*, Fig. S1 *G–L*). By monitoring the SEP-GluA2 fluorescence, we observed that an initial HFU (HFU_0) drove a long-term increase in surface GluA2 compared to baseline, as expected (Fig. 1 *F*, *G*, and *I*; 142 ± 9%, $P < 0.001$). An identical HFU stimulus at the same target spine 30 min later (HFU_{30}) induced no further GluA2 insertion (Fig. 1 *F–I*; 102 ± 4%, $P > 0.99$), despite that a second previously unstimulated, size-matched (*SI Appendix*, Fig. S1*F*) control spine on a different dendrite of the same cell exhibited a robust long-term increase in GluA2 insertion in response to HFU_{30} (Fig. 1 *F*, *H*, and *I*; 139 ± 11%, $P < 0.001$). Thus, prior potentiation initiates a refractory period for both long-term spine growth and insertion of surface AMPARs.

Refractory Period for Plasticity Is Synapse-Specific. We demonstrated that the refractory period for plasticity does not spread across the neuron to synapses on nearby dendrites; however, it remained unclear whether the refractory period is synapse-specific. As several studies demonstrate signaling interactions that influence plasticity on local dendritic segments (24, 27), we next tested whether the HFU-induced refractory period for plasticity at the target spine affected induction of plasticity at neighboring spines on the same dendritic segment (Fig. 2*A*). We stimulated a target spine with HFU to initiate long-term spine growth (Fig. 2 *B–E* and *SI Appendix*, Fig. S2 *A–C* and Table S1; 176 ± 22%; $P = 0.002$). At 40 min after the original HFU_0, we stimulated a nearby neighboring spine (within 10 µm of the target spine; average 2.9 ± 0.6 µm). We found that the nearby neighboring spine grew in response to HFU_{40} (Fig. 2 *D* and *E*; 171 ± 21%; $P = 0.004$), similarly to a size-matched (*SI Appendix*, Fig. S2*D*) control spine on different dendrites of the same cell (Fig. 2 *D* and *E*; 171 ± 21%; $P = 0.048$), demonstrating that the refractory period at target spines does not affect plasticity at nearby neighboring spines. Importantly, target spines were still fully saturated at 45 min post-HFU_0 (*SI Appendix*, Fig. S2 *F–J*). Furthermore, we did not find any correlation between the magnitude of spine growth and the distance from the HFU_0 target (*SI Appendix*, Fig. S2*E*; $P > 0.05$). These results demonstrate that the plasticity-induced refractory period at individual spines is synapse-specific.

CaMKII Activation Is Reduced in Recently Potentiated Spines. To probe the molecular mechanisms underlying the refractory period following prior potentiation, we first focused on whether CaMKII signaling is altered in recently potentiated spines. CaMKII is a key integrator of synaptic activity and plays a key regulatory role in both LTP and LTD (28–30). Using two-photon fluorescence lifetime imaging (FLIM) of Camui-α, a genetically encoded CaMKII activity reporter that exhibits increased lifetime with CaMKII activation (31), we imaged CaMKII activation (Fig. 3*A*) during and immediately following potentiation and saturation (*SI Appendix*, Fig. S3 *A–C* and Table S1) of an individual dendritic spine. In response to the initial potentiating stimulation (HFU_0), we saw a robust CaMKII activation, as detected by an increase in sensor lifetime (Fig. 3 *A–D*; 109 ± 27 ps). Notably, CaMKII activation in response to a second identical potentiating stimulus 30 min later (HFU_{30}) was robustly decreased, as evidenced by a ~60% smaller increase in CaMKII sensor lifetime (Fig. 3 *C* and *D*; 44 ± 9 ps). Peak sensor lifetime change (Fig. 3 *C* and *D*; 90 ± 14 ps) of size-matched control spines (*SI Appendix*, Fig. S3*D*) was not different than the initial response ($P = 0.54$ compared to HFU_0). Importantly, red fluorescence (*SI Appendix*, Fig. S3*E*) and donor photon counts (*SI Appendix*, Fig. S3*F*) in the target spines 25 to 30 min after HFU_0 were not different from that of size-matched control spines. A comparable decrease in CaMKII signaling 30 min after HFU was observed using a stronger stimulus that has typically been used with this sensor (31) (*SI Appendix*, Fig. S3 *G–L*). In sum, our results show that CaMKII activation is robustly reduced in recently potentiated spines.

Increased Stimulus Strength only Partially Recovers the Refractory Period for Plasticity at Previously Potentiated Spines, but Fully Recovers CaMKII Activation. We found that CaMKII activation was decreased in recently potentiated spines; therefore, we tested whether plasticity could be recovered by increasing the strength of the second stimulus to drive stronger activation of CaMKII. We therefore increased the strength of the HFU_{30} stimulus by increasing the duration of glutamate uncaging pulses from our standard 2 ms to a longer 4 ms (HFU_{30}^{+}) or 5 to 6 ms (HFU_{30}^{++}). In response to the stronger 4 ms HFU_{30}^{+} stimulation at 30 min, target spines showed a trend toward growth (Fig. 4 *A* and *B* and *SI Appendix*, Table S1; 136 ± 6% $P = 0.17$). Further increasing the strength of the second stimulation to the even stronger 5 to 6 ms HFU_{30}^{++} stimulation resulted in a nonsignificant further increase of this trend toward long-term growth (Fig. 4 *A* and *B*; 144 ± 12%, $P = 0.06$). Increasing the stimulus beyond 6 ms was not possible without damaging cell health. Notably, despite the increase in stimulus strength with HFU_{30}^{+} and HFU_{30}^{++}, the size increase of the target spine did not reach the magnitude expected from a previously unstimulated control spine receiving standard stimulation (Fig. 1*E*, reproduced in gray in Fig. 4*B*). Our results show that increasing the strength of second potentiating stimulus can partially overcome the refractory period; however, it does not fully recover plasticity to the level of spines which had not experienced prior stimulation.

Because we observed only a partial recovery of single spine plasticity with a strong stimulus, we speculated that we would see a similar partial recovery of CaMKII activation. To test this, we imaged CaMKII activity in our target spine during the first regular HFU stimulus (HFU_0) and then again at 30 min during our stronger stimulus (HFU_{30}^{+}) (Fig. 4*C*). We found that our stronger HFU_{30}^{+} stimulus was sufficient to fully recover the peak

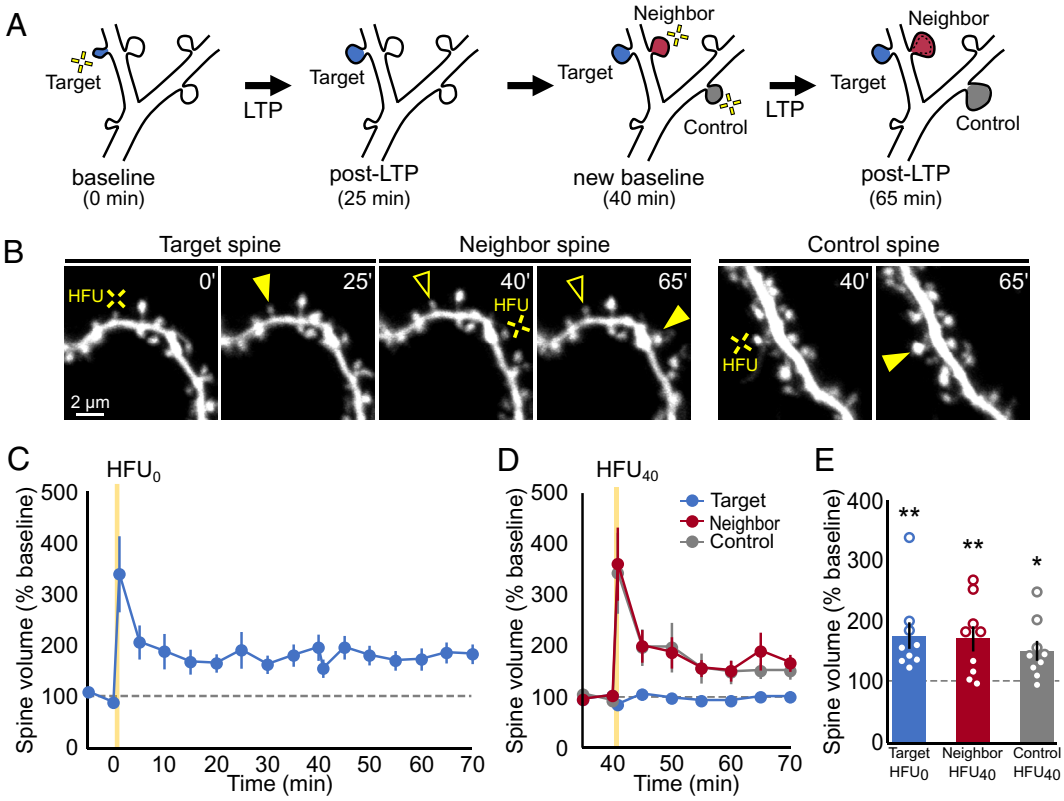

Fig. 2. Refractory period for plasticity is synapse-specific (*A*) Schematic of the experimental approach. An individual dendritic spine (target, blue) was stimulated (yellow crosses) to induce LTP and then imaged every 5 min. At 40 min, a neighbor spine (red) on the same dendrite within 10 μm of the target spine was stimulated along with a previously unstimulated, size-matched control spine (control, gray) on a different dendrite of the same cell. (*B*) Images of dendrites from an EGFP-transfected hippocampal CA1 pyramidal neuron directly prior to and 25 min after HFU_0 at target (*Left*) and HFU_{40} at neighbor (*Middle*) and control (*Right*) spines. (*C–E*) The initial HFU stimulus (HFU_0) resulted in long-term growth of target spines (filled blue circles/bars; n = 9 spines/cells), (*D*) Neighbor spine (red circles/bar; n = 9 spines/cells) and size-matched control spines (gray circles/bar; n = 9 spines/cells) grew in response to HFU_{40}. Target spine data in *D* are from *C* renormalized to the new baseline. Data are represented as mean ± SEM. Statistics: two-way ANOVA with Tukey's multiple comparisons test. **P* < 0.05, ***P* < 0.01. See also *SI Appendix*, Fig. S2.

activation of CaMKII in previously stimulated spines to levels indistinguishable from those observed in the target spine during HFU_0 and in size-matched (*SI Appendix*, Fig. S4*D*; $P = 0.29$) control spines receiving a standard HFU_{30} stimulus (Fig. 4 *C–F*; HFU_0 target: 98.0 ± 21 ps, $HFU_{30}{}^{+}$ target: 106 ± 21 ps, HFU_{30} control: 127 ± 27 ps; $P = 0.61$ and $P = 0.99$). Importantly, only partial recovery of target spine saturation was observed (*SI Appendix*, Fig. S4 *A–C*) and red fluorescence (*SI Appendix*, Fig. S4*E*) and donor photon counts (*SI Appendix*, Fig. S4*F*) in the target spines 25 to 30 min after HFU_0 was not different from that of size-matched control spines. Together, these results show that the full recovery of CaMKII activation is not sufficient to fully recover long-term spine growth, and indicate that additional mechanisms beyond CaMKII contribute to establishing the refractory period.

Refractory Period for Single Spine Plasticity Is Released within 60 min. Because a stronger stimulus was unable to fully recover plasticity of spines during the refractory period, we wondered whether full recovery from the refractory period relied on a time-dependent restoration of a vital signaling process at individual spine synapses. Prior studies at the circuit level have shown recovery of saturation of plasticity within 1 to 2 h (18, 20, 21), but some have attributed recovery to time-dependent alterations is synaptic ultrastructure (32), while others have suggested that recovery does not occur at individual synapses, but instead can be attributed to the addition of new synapses (20). We therefore examined whether recovery of plasticity could be observed at individual hippocampal CA1 synapses with a longer time interval.

To test whether increasing the time interval between the first HFU and the second HFU would permit recovery of plasticity, we repeated our experiments now with a 60 min interval between the two HFU stimuli (Fig. 5). As expected, target spines exhibited a long-term increase in size in response to the HFU_0 stimulus (Fig. 5 *A–D* and *SI Appendix*, Fig. S5 *A–C* and Table S1; 171% ± 13%, $P < 0.001$). In contrast to the lack of additional plasticity observed at 30 min, a second identical HFU stimulus at 60 min (HFU_{60}) resulted in an additional long-term increase in size of target spines (Fig. 5 *A–D*; 135% ± 11%, $P < 0.01$). Importantly, recovery of plasticity was not due to secondary effects caused by a decay in size of target spines back toward their initial value over the 60 min interval, as the long-term increase in size induced by HFU_0 was maintained for the full 60 min prior to HFU_{60} (20 to 30 min: 171 % ± 13%; 55 to 60 min: 166% ± 17%; $P = 0.8$). Furthermore, previously unstimulated, size-matched (*SI Appendix*, Fig. S5*D*) control spines on a different dendrite of the same cells grew to a comparable magnitude in response to HFU_{60} (Fig. 5 *A*, *C*, and *D*; 137% ± 9%, $P < 0.01$), supporting complete recovery of plasticity in the target spine at 60 min. Together with our prior data, our results support that the target spine was completely released from the refractory period for further plasticity between 45 to 60 min.

Increased PSD95 Expression Level Is Sufficient to Release the Refractory Period for Plasticity at Previously Potentiated Spines. Our data support the existence of a refractory period for plasticity at single spines that is released between 45 and 60 min after potentiation. In addition, because our glutamate uncaging

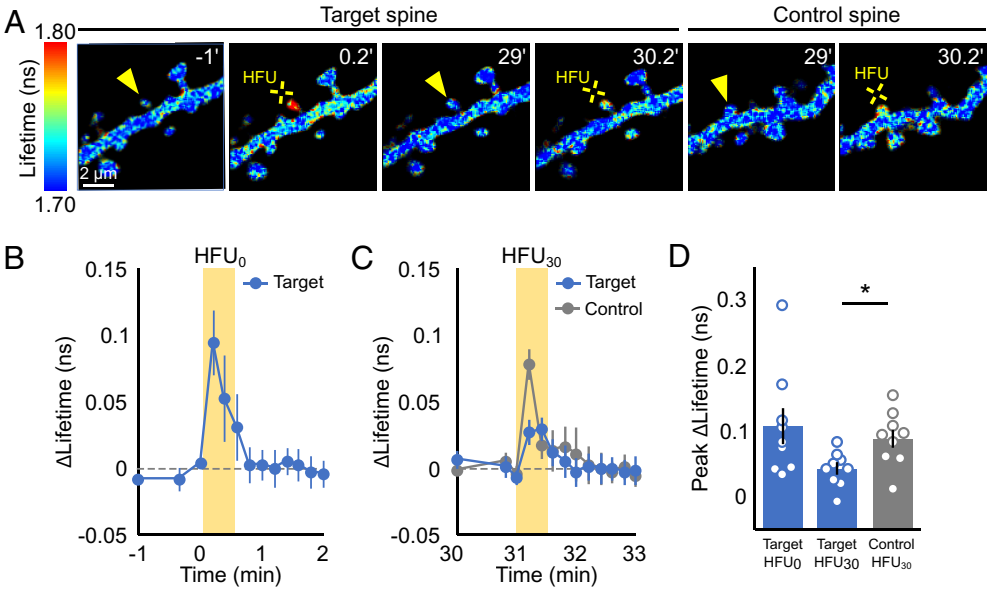

Fig. 3. CaMKII activation is reduced in previously potentiated spines (*A*) Lifetime maps from neurons in slice culture expressing CaMKII FRET sensor prior to and during high-frequency uncaging (HFU, yellow cross) at 0 min (HFU_0) and 30 min later (HFU_{30}) at target (*Left*) and control spine (*Right*). (*B*) The initial HFU stimulus (HFU_0) resulted in robust activation of CaMKII at target spines (blue circles; n = 9 spines/cells). (*C* and *D*) CaMKII activation in response to the second HFU stimulus (HFU_{30}) was reduced in previously potentiated target spines, but not in size-matched control spines (gray circles/bars; n = 9 spines/cells). Target spine data in C are from B renormalized to the new baseline. Data are represented as mean ± SEM. Statistics: paired Student's *t* test used in D. **P* < 0.05, ***P* < 0.01. See also *SI Appendix*, Fig. S3.

stimulus bypasses presynaptic vesicle release, our results support that the refractory period is initiated via postsynaptic mechanisms. Ultrastructural studies have demonstrated that the PSD of potentiated spines does not increase in size for the first 30 min after LTP induction, but does so within 2 h (33), suggesting that delayed PSD enlargement at potentiated synapses could contribute to limiting plasticity (32). Furthermore, live imaging studies have shown that the synaptic expression level of several GFP-tagged postsynaptic scaffolding proteins does not increase within 30 min of LTP induction, despite a rapid increase in spine volume (34). We therefore hypothesized that acceleration of the post-LTP PSD expansion through increasing the availability of key PSD proteins might allow for faster recovery from the refractory period. To test our hypothesis, we manipulated the expression level of PSD95, one of the most abundant PSD scaffolding proteins (35, 36) with important roles in regulating spine stabilization (37–41), and which increases at newly potentiated spines only after a delay (42).

To determine whether increased expression of PSD95 would accelerate recovery from the refractory period, we selected a 45 min time interval between the two plasticity-inducing HFU stimuli—a time at which the refractory period persisted, but such that synaptic molecular configuration would be close to recovered, and therefore increasing the expression of a single PSD protein might expedite the recovery of plasticity. CA1 neurons were transfected with GFP-tagged PSD95α (43) (PSD95-GFP) and a red cell fill (Fig. 6*A*, *Top* row). As expected, target spines exhibited a long-term increase in size in response to HFU_0 (Fig. 6 *B* and *C* and *SI Appendix*, Fig. S6*A* and Table S1; 180 ± 19%, $P < 0.001$). Notably, target spines with excess PSD95 exhibited an additional long-term increase in size in response to the second HFU at 45 min (Fig. 6 *B* and *C*; 136 ± 10%, $P < 0.05$) that was comparable to that of previously unstimulated, size-matched (*SI Appendix*, Fig. S6*B*) control spines (Fig. 6 *A* and *C*; 140% ± 13%, $P < 0.05$), suggesting complete recovery of plasticity in the target spine. Importantly, the magnitude of long-term spine growth in response to HFU_0 (*SI Appendix*, Fig. S6*C*) was not altered in cells with excess PSD95. Furthermore, increased synaptic AMPAR currents associated with excess PSD95 (44, 45) did not contribute to overcoming the refractory period, because even in the presence of NBQX to block AMPAR currents, target spines exhibited long-term growth in response to HFU_{45} (Fig. 6*D*; 148 ± 14%, $P < 0.05$), comparable to that of previously unstimulated, size-matched (*SI Appendix*, Fig. S6*D*) control spines. Thus, increased expression of PSD95 is sufficient to shorten the refractory period for plasticity induced by prior potentiation at single spines.

Increased PSD93 Expression Level does not Release the Refractory Period for Plasticity at Previously Potentiated Spines. Because PSD95 and PSD93 have extensive sequence identity [~70% overall (46)], especially in the 3 PDZ binding motifs (86%), but have distinct functional roles (47, 48), we asked whether increased PSD93 levels would also shorten the refractory period for plasticity at single spines. We therefore repeated the experiment with GFP-tagged PSD93α (44) (PSD93-GFP; Fig. 6A, *Bottom* row). In contrast to the rescue of plasticity observed with PSD95-GFP, spines from cells with excess PSD93-GFP failed to exhibit long-term growth in response to a second HFU stimulus at 45 min (Fig. 6 *E* and *F* and *SI Appendix*, Fig. S6*E*; 109 ± 7%; $P > 0.99$), despite that previously unstimulated, size-matched (*SI Appendix*, Fig. S6*F*) control spines exhibited robust growth (Fig. 6*F*; 164 ± 20%, $P < 0.05$). Importantly, spine expression of GFP-tagged proteins and initial size of the target spines were not different between PSD95- and PSD93-expressing spines (Fig. 6*G* and *SI Appendix*, Fig. S6 *G–I*). Altogether, our data show that increased expression of PSD95, but not PSD93, overcomes the refractory period for plasticity at single spines.

Discussion

That synapses which have experienced recent plasticity become temporarily resistant to further plasticity has been proposed as a mechanism through which newly formed memories can be preserved at the synaptic level while brain plasticity is ongoing (4–12). Here, we provide insights into the cellular and molecular

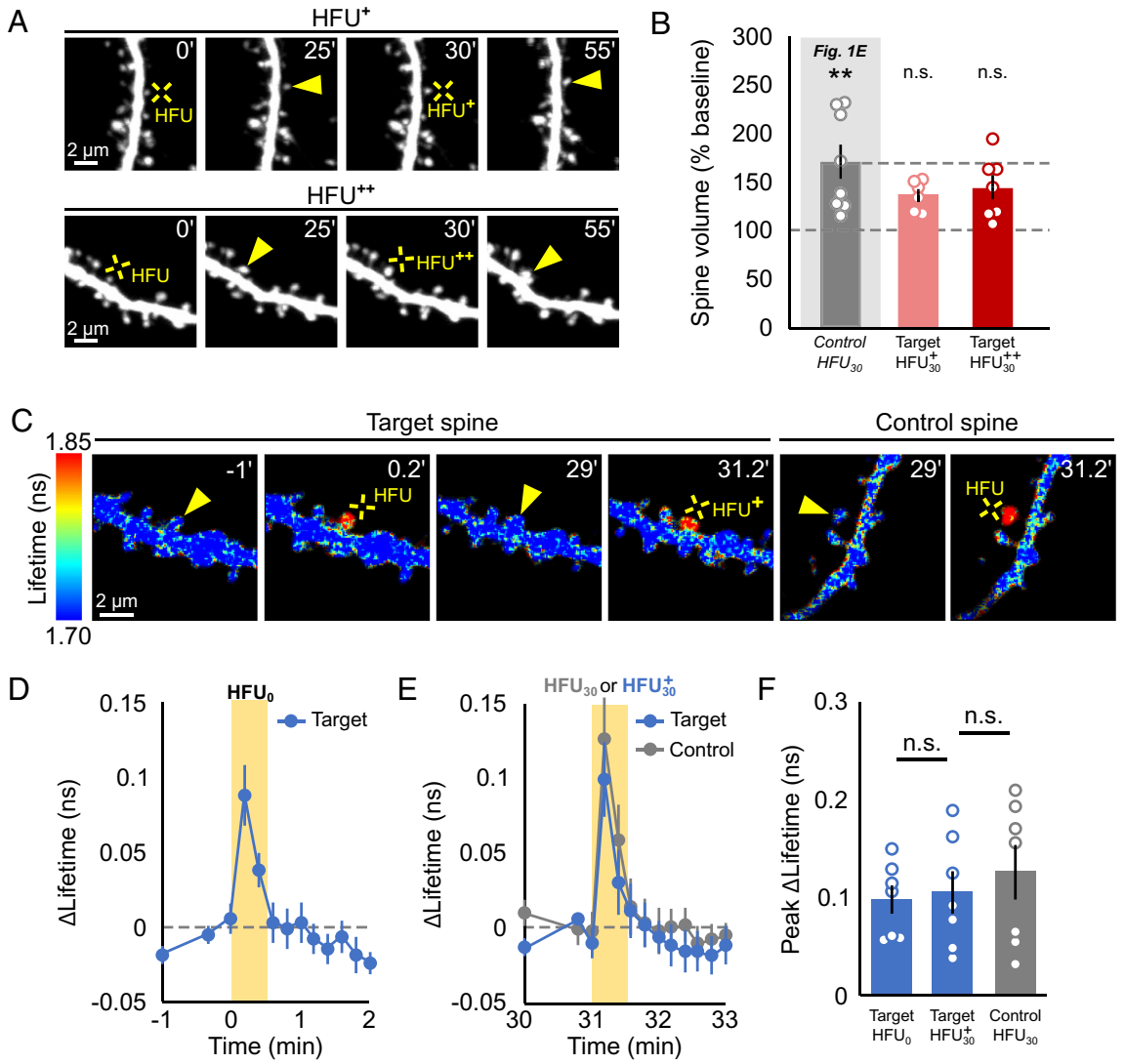

Fig. 4. Refractory period for plasticity at previously potentiated spines is only partially released by increased stimulus strength, despite full recovery of CaMKII activation (*A*) Images of spines before and after receiving HFU_0 and a stronger HFU_{30}^{+} (*Top*) or HFU_{30}^{++} (*Bottom*). (*B*) Spines exhibited a nonsignificant trend toward long-term growth in response to HFU_{30}^{+} (pink bars; n = 6 cells/spines; $P = 0.18$) and HFU_{30}^{++} (red bars; n = 7 cells/spines; $P = 0.06$). Control HFU_{30} data are replotted from Fig. 1*E*. (*C*) Lifetime maps of CaMKII in neurons from slice cultures prior to and during HFU_0 and HFU_{30}. (*D*) The initial stimulus-induced activation of CaMKII at target spines (blue circles; n = 7 spines/cells). (*E* and *F*) Stronger HFU_{30}^{+} fully recovers peak activation of CaMKII. Data are represented as mean ± SEM. Statistics: two-way ANOVA with the Bonferroni test used in B and F. *P <0.05, **P < 0.01. See also *SI Appendix*, Fig. S4.

mechanisms that regulate the establishment and duration of a refractory period for plasticity on dendrites of hippocampal CA1 neurons. We show that potentiation at single synapses is sufficient to establish a refractory period for further potentiation that is synapse-specific, lasts between 45 to 60 min, is initiated postsynaptically and accompanied by reduced postsynaptic CaMKII signaling, and is regulated by the expression level of the postsynaptic scaffolding protein, PSD95, but not by PSD93.

Initiation, Time-Course, and Synapse-Specificity of Refractory Period for Potentiation. We demonstrate that a single LTP-inducing glutamatergic stimulus at an individual spine is sufficient to initiate a refractory period for further structural and functional potentiation. Earlier studies established that this type of metaplasticity, or "saturation of plasticity" is observed at the circuit level (18–21). Here, we show that the signaling mechanisms needed to establish the refractory period can be activated locally at single synapses, and do not require activating multiple axons as in circuit-level studies using a variety of protocols to induce LTP, including tetanic, theta-burst, and pairing stimulation (18–21). Importantly, because our glutamate uncaging stimulation bypasses presynaptic vesicle release, our results point to a postsynaptic locus of initiation for the refractory period. We further show that the refractory period for further potentiation is restricted to the potentiated spine; it is not observed at previously unstimulated, size-matched control spines within 10 µm of the target spine on the same dendritic segment, supporting that the refractory period is synapse-specific.

Because our experimental paradigm focused on single synapses, we were able to distinguish that full recovery can occur at these hippocampal CA1 synapses without the need to recruit additional naïve synapses (18), although our results do not exclude that such mechanisms are in operation. It is likely that the success of induction and duration of the refractory period will be dependent on the pattern, strength, and extent of synaptic activity at single synapses. Indeed, it has been recently reported that different naturalistic patterns of activity influence the duration of long-term synaptic structural plasticity (49).

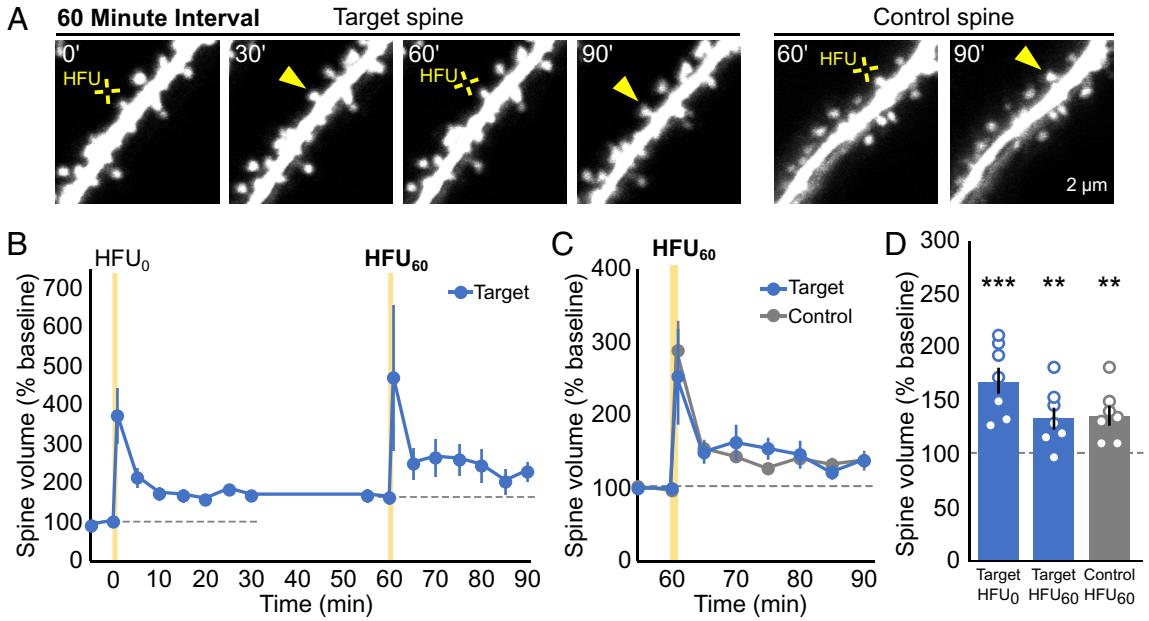

Fig. 5. Refractory period for plasticity at previously potentiated spines is released within 60 min (*A*) Images of dendrites from an EGFP-transfected CA1 neuron in slice culture directly prior to and 30 min after HFU_0 and HFU_{60} at target and control spines. (*B–D*) A second HFU at 60 min (HFU_{60}) resulted in additional growth (filled blue circles/bars, n = 7 spines/cells), comparable to that observed from size-matched control spines on the same cell (gray circles/bar; n = 7 spines/cells). Target spine data in *C* are from *B* renormalized to the new baseline. Data are represented as mean ± SEM. Statistics: two-way ANOVA with the Bonferroni test. $*P < 0.05$, $**P < 0.01$. See also *SI Appendix*, Fig. S5.

Molecular Mechanisms of Refractory Period for Potentiation. We show that CaMKII activation is reduced in recently potentiated spines, relative both to initial activation in the same spines following induction of LTP, and to activation in size-matched control spines on different dendrites of the same neuron. How might CaMKII activation levels be reduced specifically in recently potentiated spines? It is possible that the reduction in CaMKII activity is due to the local upregulation of endogenous CaMKII inhibitors, such as CaMKII inhibitor 1 (CaMK2N1), which has been shown to be upregulated after the induction of LTP (50). Another possibility would be through mechanisms that drive reduced calcium influx following LTP. For example, a local feedback loop between the NMDA receptor and the Ca^{2+}-activated small conductance potassium channel, SK2, could lead to a local reduction in the NMDAR Ca^{2+} currents (51). In addition, spine calcium handling is influenced by changes in the ER that can regulate the efficacy of spine structural plasticity (52, 53). Alternatively, activity (54–56) and the induction of LTP (57) have been shown to drive a rapid change from GluN2B- to GluN2A-containing NMDARs, which carry less Ca^{2+} current and are less favorable to induction of LTP (57, 58). This switch is likely to occur also at single synapses, as prolonged inactivation of synaptic transmission at individual synapses on cultured hippocampal neurons induces the opposite switch from GluN2A to GluN2B (59). However, in at least some reports (59), the LTP-induced subunit switch shows no recovery within one hour and it is not observed in slices from older animals comparable in age to those used for our experiments. Regardless of the cause of reduced CaMKII activation, we show that recovery of CaMKII activation in spines during the refractory period is not sufficient to drive plasticity, consistent with studies showing that a photoactivatable CaMKII cannot further induce long-term spine growth in recently potentiated spines (60).

We found that increased levels of the postsynaptic scaffolding protein PSD95 restored plasticity to recently potentiated synapses in the refractory period. Our results suggest that lower levels of PSD95 in recently potentiated synapses contribute to establishment or maintenance of the refractory period. Indeed, ultrastructural studies following the induction of LTP have demonstrated that the PSD takes between 30 min and 2 h to grow (33), and molecular imaging studies have established that PSD-scaffolding molecules, including PSD95, accumulate to steady-state levels only after a delay of more than 30 min (34). Intriguingly, we show that increased expression of PSD93, which is also at low levels following LTP, is not sufficient to restore plasticity to recently potentiated synapses. This might be viewed as surprising, as these two PSD-MAGUKs have a high degree of sequence identity, and share 3 PDZ domains, an SH3, and a GK domain with 2 palmitoylation sites (61), and both have demonstrated roles in spine stabilization (37–41). However, despite the similarities, PSD95 and PSD93 have many distinct physiological roles. For example, homeostatic upscaling of synaptic currents requires both PSD95 and PSD93, while scaling down does not require PSD93 (47). In addition, loss of PSD95 prevents maturation of silent synapses, while loss of PSD93 has the opposite effect, instead leading to accelerated maturation of silent synapses (48). Furthermore, in nascent dendritic spines, PSD93 is enriched to mature levels within several hours, whereas PSD95 takes over 12 h to reach mature levels, suggesting sequential roles in nascent spine stabilization (62).

How might PSD95 levels regulate the refractory period? Our results provide experimental evidence in support of models based on ultrastructural studies positing that delayed expansion of the PSD limits further potentiation at recently potentiated synapses (32). In these models, it has been proposed that the refractory period ends via the expansion of nascent zones, regions of the presynaptic bouton that lack glutamate release machinery but are apposed to the PSD (32). Our results are consistent with a model in which excess PSD95 is sufficient to drive expansion of the PSD and addition of nascent zones, and thus recovery of plasticity. Alternatively, PSD95 could rescue the refractory period by inhibiting signaling that leads to the refractory period. Molecularly, reduced PSD95 levels following LTP would be expected to permit increased levels of $STEP_{61}$, a tyrosine phosphatase that targets GluN2B for endocytosis (63), and thus would act to reduce the

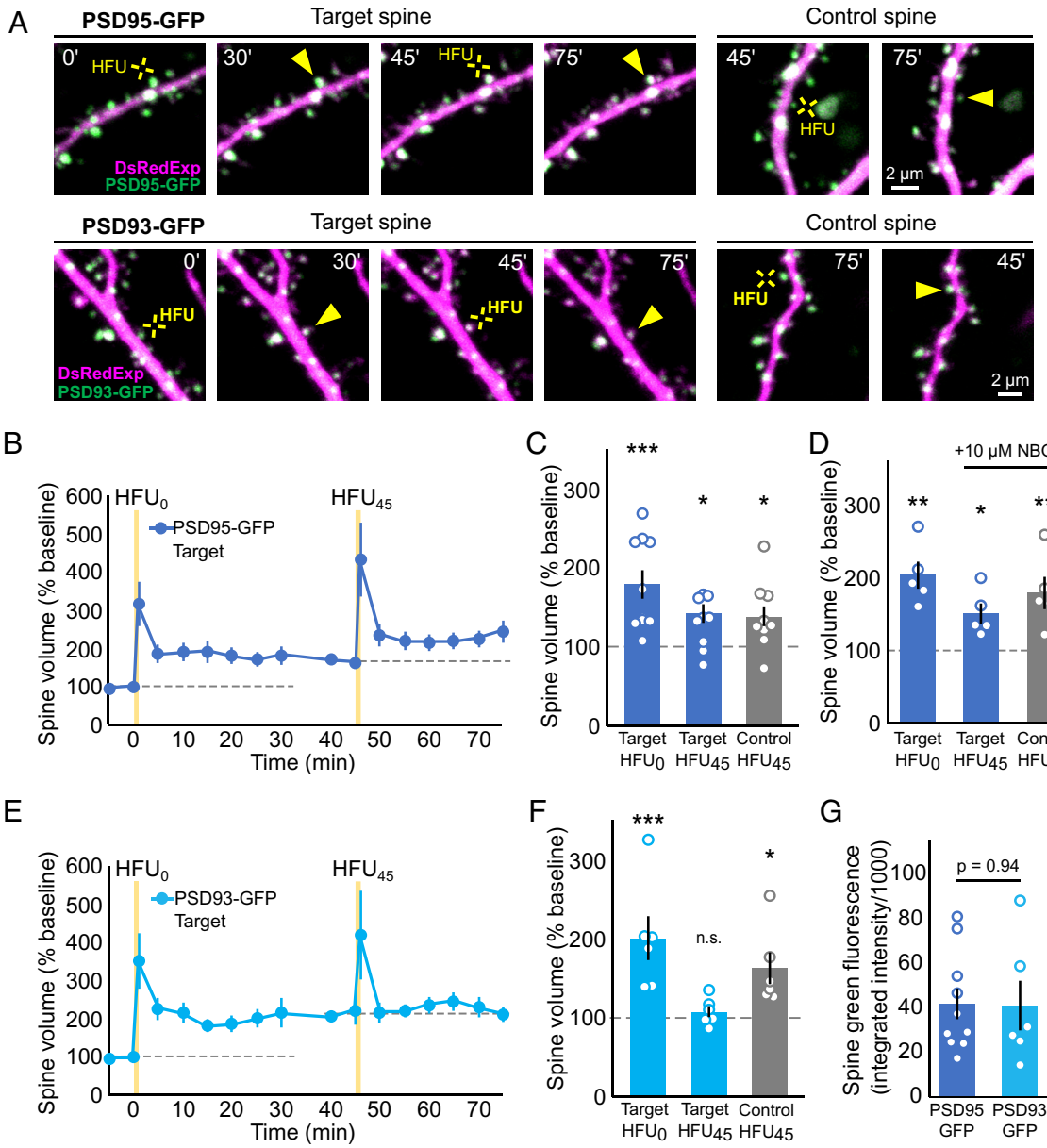

Fig. 6. Increased availability of PSD95, but not PSD93, restores plasticity to spines in the refractory period (*A*) Images of dendrites from CA1 pyramidal neurons transfected with DsRedExpress (magenta) and PSD95-GFP (green; *Top* row) or PSD93-GFP (green; *Bottom* row) directly prior to and 30 min after HFU_0 and HFU_{45} at target and control spines. (*B* and *C*) PSD95-GFP-expressing target spines grew in response to a second HFU at 45 min (HFU_{45}) (dark blue circles/bars; n = 10 spines/cells, $P < 0.05$), even when (*D*) NBQX was added to block current through AMPARs (n = 5 spines/cells). (*E* and *F*) In contrast, PSD93-expressing target spines did not grow in response to HFU_{45} (light blue circles/bar; n = 6 spines/cells; $P > 0.99$). (*G*) Expression levels of PSD95-GFP and PSD93-GFP were comparable. Data are represented as mean ± SEM. Statistics: two-way ANOVA with the Bonferroni test used in *C*, *D*, and *F*; unpaired Student's *t* test used in *G*. $*P < 0.05$, $***P < 0.001$. See also *SI Appendix*, Fig. S6.

efficacy of LTP until the return of PSD95, exclusion of $STEP_{61}$, and subsequent return of GluN2B levels (54).

Implications for Learning of Refractory Period for Plasticity. A refractory period for plasticity during learning at recently potentiated synapses would serve an important role to exclude those synapses from incorporation into distinct subsequently learned tasks, thus preventing overwriting of recently established memories still in the labile phase (4–8, 12). It could also play a role in preventing runaway plasticity, in which potentiated synapses drive increased action potential firing and thus generate a feedback loop of potentiation (64). Another consequence of a refractory period on learning would be to temporarily prevent synapses from undergoing further potentiation related to the same task. Indeed, there is considerable evidence that repeated learning bouts activate the same sets of synapses (2, 65, 66). Several have proposed that a refractory period for plasticity could be the basis for increased success of a type of learning known as spaced learning, in which breaks are incorporated into learning sessions (20, 32). Such breaks during spaced learning could serve to allow synapses to recover their ability to undergo plasticity. Indeed, spaced learning approaches have been shown to improve learning outcomes over traditional learning in which repetitions are temporally clustered in both humans and rodents (65, 67, 68), and to improve learning under conditions where learning is challenged in disease (69, 70). It follows that manipulation of the molecular signaling mechanisms that regulate the refractory period could serve to improve learning outcomes associated with disease.

Materials and Methods

Preparation and Transfection of Organotypic Hippocampal Slice Cultures. Cultured hippocampal slices (300 to 400 μm) were prepared from P6-P8 C57BL/6 mice of both sexes, as described (71), and as approved by the UC Davis Institutional Animal Care and Use Committee. Slices were transfected at 9 to 15 DIV using biolistic gene transfer (180 to 210 psi), as described (72). 6 to 8 mg of 1.6 μm gold beads (BioRad) were coated with 15 μg of EGFP-N1 (Clontech), or 10 μg of tDimer-dsRed together with 16 μg SEP-GluA2 (26), or 30 μg of green-Camui-α (Addgene #26933) together with 10 μg of CyRFP1 (Addgene #84356), or 10 μg of DsRedExpress (Clontech) alone or 10 μg DsRedExpress together with 1 to 2 μg of GFP-tagged PSD95α (43) or PSD93α (44). Slices were transfected 2 to 3 d (EGFP or green-Camui-α/CyRFP), 3 to 4 d (SEP-GluA2/tDimer-dsRed), or 24 h (PSD95/93/DsRedExpress) prior to imaging.

Time-Lapse Two-Photon Imaging. Transfected CA1 pyramidal neurons at depths of 10 to 50 μm in slice cultures (11 to 17 DIV) were imaged using a custom two-photon microscope (73) controlled with ScanImage (74). Image stacks (512 x 512 pixels; 0.02 μm/pixel) with 1 μm z-steps were collected. For each neuron, one segment of secondary or tertiary basal dendrite was selected under epifluorescence and imaged at 5 min intervals at 29 °C in recirculating ACSF (in mM): 127 NaCl, 25 $NaHCO_3$, 1.2NaH_2PO_4, 2.5 KCl, 25 D-glucose, aerated with 95% O_2/5% CO_2, 310 mOsm, pH 7.2, with 0.001 TTX, 0 Mg^{2+}, and 2 Ca^{2+}. MNI-glutamate (2.5 mM; Tocris) was added at least 15 min prior to uncaging stimulation.

High-Frequency Uncaging (HFU) of Glutamate. HFU consisted of 60 pulses (720 nm; ~7.5 to 9.5 mW at the sample) of 2 ms duration (4 ms for HFU^{+}, 5 to 6 ms for HFU^{++}) at 2 Hz delivered in ACSF containing (in mM): 2 Ca^{2+}, 0 Mg^{2+}, 2.5 MNI-glutamate, and 0.001 TTX. Because earlier studies established that spine size can influence the magnitude of potentiation (22), we selected target spines with an initial size range in the 25 to 50% quartile of sizes. The laser beam was parked at a point ~0.5 to 1 μm from the spine head in the direction away from the dendrite. Cells with no noticeable transients in response to HFU_0 were discarded and not further pursued.

Image Analysis. Images were analyzed using a custom MATLAB software, as described (73). In brief, following application of a 3 × 3 median filter, background-subtracted integrated green and/or red fluorescence intensity was calculated from a boxed region surrounding the spine head. Spine volume was estimated using fluorescence from a cell fill (EGFP, tDimer-dsRed, or DsRedExpress) (75). Bar graphs show the average values from the three time points occurring at 20 to 30 min after the most recent HFU (HFU_0: 20 to 30 min; HFU_{30}: 50 to 60 min; HFU_{40}: 60 to 70 min; HFU_{45}: 65 to 75 min; HFU_{60}: 80 to 90 min). Relative spine size was calculated by normalizing the individual spine fluorescence to the mean for all spines on the same dendrite using the two time points immediately prior to HFU.

Two-Photon FLIM. Fluorescence lifetime was measured using a custom two-photon microscope with time-correlated single photon counting (Becker-Hickl) and GaAs(P) detectors (H7422PA-40; Hamamatsu). Images (24 frame scans; 128 × 128; 0.7 μm per pixel) were acquired and data was analyzed using custom MATLAB software developed in the laboratory of Dr. Ryohei Yasuda, as previously described (76). CaMKII activity was measured as the lifetime change of the sensor from baseline (average of 6 min prior to HFU) at each time point (ΔLifetime).

Statistics. All data are represented as mean ± SEM. All statistics were calculated across cells using GraphPad Prism. Statistical significance level (α) was set to $P < 0.05$ for all tests. When comparing only two groups, paired or unpaired (as appropriate) Student's t-tests were used. When multiple comparisons were made, a one or two-way ANOVA with the Bonferroni post hoc test was performed. All *P* values are in the text and n values are in the figure legends.

Data, Materials, and Software Availability. All study data are included in the article and/or *SI Appendix*. All raw image files and analysis files are available at Dryad (DOI: 10.5061/dryad.ghx3ffc0b) (77).

ACKNOWLEDGMENTS. This work was supported by the NIH (R01 NS062736, R56 MH139176). J.C.F. was additionally supported by an NIH training grant (T32 GM099608), NIH D-SPAN Award (F99 NS125772), and an ARCS fellowship. We thank Ryohei Yasuda for generously providing FLIM microscope setup design and custom FLIM software; J. Jahncke and L. Tom for support with experiments; J. Hell, J. Gray, J. Zheng, M. Navedo, I. Stein, S. Petshow, M. Anisimova; and M. Alarcon for critical input and/or reading of the manuscript. An earlier submitted version of this paper with J.C.F. and K.Z. as coauthors was included as a chapter in the PhD thesis of J.C.F.

1. J. Grutzendler, N. Kasthuri, W.-B. Gan, Long-term dendritic spine stability in the adult cortex. *Nature* **420**, 812–816 (2002), 10.1038/nature01276.
2. A. Hayashi-Takagi *et al.*, Labelling and optical erasure of synaptic memory traces in the motor cortex. *Nature* **525**, 333–338 (2015), 10.1038/nature15257.
3. J. T. Trachtenberg *et al.*, Long-term in vivo imaging of experience-dependent synaptic plasticity in adult cortex. *Nature* **420**, 788–794 (2002), 10.1038/nature01273.
4. W. C. Abraham, O. D. Jones, D. L. Glanzman, Is plasticity of synapses the mechanism of long-term memory storage? *NPJ Sci. Learn.* **4**, 9 (2019), 10.1038/s41539-019-0048-y.
5. C. H. Bailey, E. R. Kandel, K. M. Harris, Structural components of synaptic plasticity and memory consolidation. *Cold Spring Harb Perspect Biol* **7**, a021758 (2015), 10.1101/cshperspect.a021758.
6. T. V. P. Bliss, G. L. Collingridge, A synaptic model of memory: Long-term potentiation in the hippocampus. *Nature* **361**, 31–39 (1993), 10.1038/361031a0.
7. J. C. Magee, C. Grienberger, Synaptic plasticity forms and functions. *Annu. Rev. Neurosci.* **43**, 95–117 (2020), 10.1146/annurev-neuro-090919-022842.
8. S. J. Martin, P. D. Grimwood, R. G. M. Morris, Synaptic plasticity and memory: An evaluation of the hypothesis. *Annu. Rev. Neurosci.* **23**, 649–711 (2000), 10.1146/annurev.neuro.23.1.649.
9. G. Mongillo, S. Rumpel, Y. Loewenstein, Intrinsic volatility of synaptic connections–a challenge to the synaptic trace theory of memory. *Curr. Opin. Neurobiol.* **46**, 7–13 (2017), 10.1016/j.conb.2017.06.006.
10. R. Chaudhuri, I. Fiete, Computational principles of memory. *Nat. Neurosci.* **19**, 394–403 (2016), 10.1038/nn.4237.
11. H. Kasai *et al.*, Spine dynamics in the brain, mental disorders and artificial neural networks. *Nat. Rev. Neurosci.* **22**, 407–422 (2021), 10.1038/s41583-021-00467-3.
12. S. Fusi, P. J. Drew, L. F. Abbott, Cascade models of synaptically stored memories. *Neuron* **45**, 599–611 (2005), 10.1016/j.neuron.2005.02.001.
13. G. M. Van De Ven *et al.*, Three types of incremental learning. *Nat. Mach. Intell.* **4**, 1185–1197 (2022), 10.1038/s42256-022-00568-3.
14. G. M. Van De Ven *et al.*, Brain-inspired replay for continual learning with artificial neural networks. *Nat. Commun.* **11**, 4069 (2020), 10.1038/s41467-020-17866-2.
15. M. Fu, X. Yu, J. Lu, Y. Zuo, Repetitive motor learning induces coordinated formation of clustered dendritic spines in vivo. *Nature* **483**, 92–95 (2012), 10.1038/nature10844.
16. C. Barnes *et al.*, LTP saturation and spatial learning disruption: Effects of task variables and saturation levels. *J. Neurosci.* **14**, 5793–5806 (1994), 10.1523/JNEUROSCI.14-10-05793.1994.
17. E. I. Moser, Impaired spatial learning after saturation of long-term potentiation. *Science* **281**, 2038–2042 (1998), 10.1126/science.281.5385.2038.
18. Y. Huang, A. Colino, D. Selig, R. Malenka, The influence of prior synaptic activity on the induction of long-term potentiation. *Science* **255**, 730–733 (1992), 10.1126/science.1346729.
19. U. Frey, K. Schollmeier, K. G. Reymann, T. Seidenbecher, Asymptotic hippocampal long-term potentiation in rats does not preclude additional potentiation at later phases. *Neuroscience* **67**, 799–807 (1995), 10.1016/0306-4522(95)00117-2.
20. E. A. Kramar *et al.*, Synaptic evidence for the efficacy of spaced learning. *Proc. Natl. Acad. Sci. U.S.A.* **109**, 5121–5126 (2012), 10.1073/pnas.1120700109.
21. G. Cao, K. M. Harris, Augmenting saturated LTP by broadly spaced episodes of theta-burst stimulation in hippocampal area CA1 of adult rats and mice. *J. Neurophysiol.* **112**, 1916–1924 (2014), 10.1152/jn.00297.2014.
22. M. Matsuzaki, N. Honkura, G. C. R. Ellis-Davies, H. Kasai, Structural basis of long-term potentiation in single dendritic spines. *Nature* **429**, 761–766 (2004), 10.1038/nature02617.
23. T. C. Hill, K. Zito, LTP-induced long-term stabilization of individual nascent dendritic spines. *J. Neurosci.* **33**, 678–686 (2013), 10.1523/JNEUROSCI.1404-12.2013.
24. W. C. Oh, L. K. Parajuli, K. Zito, Heterosynaptic structural plasticity on local dendritic segments of hippocampal CA1 neurons. *Cell Rep.* **10**, 162–169 (2015), 10.1016/j.celrep.2014.12.016.
25. G. Miesenböck, D. A. De Angelis, J. E. Rothman, Visualizing secretion and synaptic transmission with pH-sensitive green fluorescent proteins. *Nature* **394**, 192–195 (1998), 10.1038/28190.
26. C. D. Kopec, B. Li, W. Wei, B. Jannic, M. Roberto, Glutamate receptor exocytosis and spine enlargement during chemically induced long-term potentiation. *J. Neurosci.* **26**, 2000–2009 (2006), 10.1523/JNEUROSCI.3918-05.2006.
27. C. D. Harvey, K. Svoboda, Locally dynamic synaptic learning rules in pyramidal neuron dendrites. *Nature* **450**, 1195–1200 (2007), 10.1038/nature06416.
28. K. U. Bayer, H. Schulman, CaM kinase: Still inspiring at 40. *Neuron* **103**, 380–394 (2019), 10.1016/j.neuron.2019.05.033.
29. R. Yasuda, Y. Hayashi, J. W. Hell, CaMKII: A central molecular organizer of synaptic plasticity, learning and memory. *Nat. Rev. Neurosci.* **23**, 666–682 (2022), 10.1038/s41583-022-00624-2.
30. S. G. Cook, O. R. Buonarati, S. J. Coultrap, K. U. Bayer, CaMKII holoenzyme mechanisms that govern the LTP versus LTD decision. *Sci. Adv.* **7**, eabe2300 (2021), 10.1126/sciadv.abe2300.
31. S.-J.R. Lee, Y. Escobedo-Lozoya, E. M. Szatmari, R. Yasuda, Activation of CaMKII in single dendritic spines during long-term potentiation. *Nature* **458**, 299–304 (2009), 10.1038/nature07842.
32. M. E. Bell *et al.*, Dynamics of nascent and active zone ultrastructure as synapses enlarge during long-term potentiation in mature hippocampus: Nascent and active zone structural dynamics. *J. Comp. Neurol.* **522**, 3861–3884 (2014), 10.1002/cne.23646.
33. J. N. Bourne, K. M. Harris, Coordination of size and number of excitatory and inhibitory synapses results in a balanced structural plasticity along mature hippocampal CA1 dendrites during LTP. *Hippocampus* **21**, 354–373 (2011), 10.1002/hipo.20768.
34. M. Bosch *et al.*, Structural and molecular remodeling of dendritic spine substructures during long-term potentiation. *Neuron* **82**, 444–459 (2014), 10.1016/j.neuron.2014.03.021.

35. K.-O. Cho, C. A. Hunt, M. B. Kennedy, The rat brain postsynaptic density fraction contains a homolog of the drosophila discs-large tumor suppressor protein. *Neuron* **9**, 929–942 (1992), 10.1016/0896-6273(92)90245-9.
36. M. B. Kennedy, The postsynaptic density at glutamatergic synapses. *Trends Neurosci.* **20**, 264–268 (1997), 10.1016/S0166-2236(96)01033-8.
37. S. Okabe, A. Miwa, H. Okado, Spine formation and correlated assembly of presynaptic and postsynaptic molecules. *J. Neurosci.* **21**, 6105–6114 (2001), 10.1523/JNEUROSCI.21-16-06105.2001.
38. I. Ehrlich, M. Klein, S. Rumpel, R. Malinow, PSD-95 is required for activity-driven synapse stabilization. *Proc. Natl. Acad. Sci. U.S.A.* **104**, 4176–4181 (2007), 10.1073/pnas.0609307104.
39. M. De Roo, P. Klauser, P. Mendez, L. Poglia, D. Muller, Activity-dependent PSD formation and stabilization of newly formed spines in hippocampal slice cultures. *Cereb. Cortex* **18**, 151–161 (2008), 10.1093/cercor/bhm041.
40. C. E. Taft, G. G. Turrigiano, PSD-95 promotes the stabilization of young synaptic contacts. *Phil. Trans. R. Soc. B* **369**, 20130134 (2014), 10.1098/rstb.2013.0134.
41. M. Cane, B. Maco, G. Knott, A. Holtmaat, The relationship between PSD-95 clustering and spine stability in vivo. *J. Neurosci.* **34**, 2075–2086 (2014), 10.1523/JNEUROSCI.3353-13.2014.
42. D. Meyer, T. Bonhoeffer, V. Scheuss, Balance and stability of synaptic structures during synaptic plasticity. *Neuron* **82**, 430–443 (2014), 10.1016/j.neuron.2014.02.031.
43. N. W. Gray, R. M. Weimer, I. Bureau, K. Svoboda, Rapid redistribution of synaptic PSD-95 in the neocortex in vivo. *PLoS Biol.* **4**, e370 (2006), 10.1371/journal.pbio.0040370.
44. E. Schnell *et al.*, Direct interactions between PSD-95 and stargazin control synaptic AMPA receptor number. *Proc. Natl. Acad. Sci. U.S.A.* **99**, 13902–13907 (2002), 10.1073/pnas.172511199.
45. I. Ehrlich, R. Malinow, Postsynaptic density 95 controls AMPA receptor incorporation during long-term potentiation and experience-driven synaptic plasticity. *J. Neurosci.* **24**, 916–927 (2004), 10.1523/JNEUROSCI.4733-03.2004.
46. J. E. Brenman, K. S. Christopherson, S. E. Craven, A. W. McGee, D. S. Bredt, Cloning and characterization of postsynaptic density 93, a nitric oxide synthase interacting protein. *J. Neurosci.* **16**, 7407–7415 (1996), 10.1523/JNEUROSCI.16-23-07407.1996.
47. Q. Sun, G. G. Turrigiano, PSD-95 and PSD-93 play critical but distinct roles in synaptic scaling up and down. *J. Neurosci.* **31**, 6800–6808 (2011), 10.1523/JNEUROSCI.5616-10.2011.
48. P. D. Favaro *et al.*, An opposing function of paralogs in balancing developmental synapse maturation. *PLoS Biol.* **16**, e2006838 (2018), 10.1371/journal.pbio.2006838.
49. A. Ö. Argunsah, I. Israely, The temporal pattern of synaptic activation determines the longevity of structural plasticity at dendritic spines. *iScience* **26**, 106835 (2023), 10.1016/j.isci.2023.106835.
50. D. Astudillo *et al.*, CaMKII inhibitor 1 (CaMK2N1) mRNA is upregulated following LTP induction in hippocampal slices. *Synapse* **74**, e22158 (2020), 10.1002/syn.22158.
51. T. J. Ngo-Anh *et al.*, SK channels and NMDA receptors form a Ca2+-mediated feedback loop in dendritic spines. *Nat. Neurosci.* **8**, 642–649 (2005), 10.1038/nn1449.
52. P. J. Dittmer, M. L. Dell'Acqua, L-type Ca 2+ channel activation of STIM1–Orai1 signaling remodels the dendritic spine ER to maintain long-term structural plasticity *Proc. Natl. Acad. Sci. U.S.A.* **121**, e2407324121 (2024), 10.1073/pnas.2407324121.
53. A. Perez-Alvarez *et al.*, Endoplasmic reticulum visits highly active spines and prevents runaway potentiation of synapses. *Nat. Commun.* **11**, 5083 (2020), 10.1038/s41467-020-18889-5.
54. A. Sanz-Clemente, J. A. Matta, J. T. R. Isaac, K. W. Roche, Casein kinase 2 regulates the NR2 subunit composition of synaptic NMDA receptors. *Neuron* **67**, 984–996 (2010), 10.1016/j.neuron.2010.08.011.
55. J. A. Matta *et al.*, mGluR5 and NMDA receptors drive the experience- and activity-dependent NMDA receptor NR2B to NR2A subunit switch. *Neuron* **70**, 339–351 (2011), 10.1016/j.neuron.2011.02.045.
56. Z. Xu *et al.*, Metaplastic regulation of long-term potentiation/long-term depression threshold by activity-dependent changes of NR2A/NR2B ratio. *J. Neurosci.* **29**, 8764–8773 (2009), 10.1523/JNEUROSCI.1014-09.2009.
57. C. Bellone, R. A. Nicoll, Rapid bidirectional switching of synaptic NMDA receptors. *Neuron* **55**, 779–785 (2007), 10.1016/j.neuron.2007.07.035.
58. P. Paoletti, C. Bellone, Q. Zhou, NMDA receptor subunit diversity: Impact on receptor properties, synaptic plasticity and disease. *Nat. Rev. Neurosci.* **14**, 383–400 (2013), 10.1038/nrn3504.
59. M.-C. Lee, R. Yasuda, M. D. Ehlers, Metaplasticity at single glutamatergic synapses. *Neuron* **66**, 859–870 (2010), 10.1016/j.neuron.2010.05.015.
60. H. H. Ueda *et al.*, Chronic neuronal excitation leads to dual metaplasticity in the signaling for structural long-term potentiation. *Cell Rep.* **38**, 110153 (2022), 10.1016/j.celrep.2021.110153.
61. S. Won, J. M. Levy, R. A. Nicoll, K. W. Roche, MAGUKs: Multifaceted synaptic organizers. *Curr. Opin. Neurobiol.* **43**, 94–101 (2017), 10.1016/j.conb.2017.01.006.
62. J. T. Lambert *et al.*, Protracted and asynchronous accumulation of PSD95-family MAGUKs during maturation of nascent dendritic spines: Accumulation of PSD-MAGUKs in new spines. *Dev. Neurobiol.* **77**, 1161–1174 (2017), 10.1002/dneu.22503.
63. S. Won, S. Incontro, R. A. Nicoll, K. W. Roche, PSD-95 stabilizes NMDA receptors by inducing the degradation of STEP 61. *Proc. Natl. Acad. Sci. U.S.A.* **113**, E4736–E4744 (2016), 10.1073/pnas.1609702113.
64. J.-Y. Chen *et al.*, Heterosynaptic plasticity prevents runaway synaptic dynamics. *J. Neurosci.* **33**, 15915–15929 (2013), 10.1523/JNEUROSCI.5088-12.2013.
65. A. Glas, M. Hübener, T. Bonhoeffer, P. M. Goltstein, Spaced training enhances memory and prefrontal ensemble stability in mice. *Curr. Biol.* **31**, 4052–4061.e6 (2021), 10.1016/j.cub.2021.06.085.
66. S. B. Hofer, T. D. Mrsic-Flogel, T. Bonhoeffer, M. Hübener, Experience leaves a lasting structural trace in cortical circuits. *Nature* **457**, 313–317 (2009), 10.1038/nature07487.
67. M. Boettcher *et al.*, The spaced learning concept significantly improves training for laparoscopic suturing: A pilot randomized controlled study. *Surg. Endosc.* **32**, 154–159 (2018), 10.1007/s00464-017-5650-6.
68. P. Smolen, Y. Zhang, J. H. Byrne, The right time to learn: Mechanisms and optimization of spaced learning. *Nat. Rev. Neurosci.* **17**, 77–88 (2016), 10.1038/nrn.2015.18.
69. J. C. Lauterborn *et al.*, Spaced training improves learning in Ts65Dn and Ube3a mouse models of intellectual disabilities. *Transl. Psychiatry* **9**, 166 (2019), 10.1038/s41398-019-0495-5.
70. R. R. Seese *et al.*, Spaced training rescues memory and ERK1/2 signaling in fragile X syndrome model mice. *Proc. Natl. Acad. Sci. U.S.A.* **111**, 16907–16912 (2014), 10.1073/pnas.1413335111.
71. L. Stoppini, P.-A. Buchs, D. Muller, A simple method for organotypic cultures of nervous tissue. *J. Neurosci. Methods* **37**, 173–182 (1991), 10.1016/0165-0270(91)90128-M.
72. G. Woods, K. Zito, Preparation of gene gun bullets and biolistic transfection of neurons in slice culture. *J. Vis. Exp.* **12**, 675 (2008), 10.3791/675.
73. G. F. Woods *et al.*, Loss of PSD-95 enrichment is not a prerequisite for spine retraction. *J. Neurosci.* **31**, 12129–12138 (2011), 10.1523/JNEUROSCI.6662-10.2011.
74. T. A. Pologruto, B. L. Sabatini, K. Svoboda, ScanImage: Flexible software for operating laser scanning microscopes. *Biomed. Eng. Online* **2**, 13 (2003), 10.1186/1475-925X-2-13.
75. A. J. G. D. Holtmaat *et al.*, Transient and persistent dendritic spines in the neocortex in vivo. *Neuron* **45**, 279–291 (2005), 10.1016/j.neuron.2005.01.003.
76. R. Yasuda, Imaging spatiotemporal dynamics of neuronal signaling using fluorescence resonance energy transfer and fluorescence lifetime imaging microscopy. *Curr. Opin. Neurobiol.* **16**, 551–561 (2006), 10.1016/j.conb.2006.08.012.
77. J. Flores, D. Sarkar, K. Zito, Data from "A synapse-specific refractory period for plasticity at individual dendritic spines". Dryad. https://doi.org/10.5061/dryad.ghx3ffc0b. Deposited 20 December 2024.